INTERACTION FORCES BETWEEN TONER SURFACES

Maria A. D. Azevedo
Graduate Student
University of Utah
Salt Lake City, UT 84112
U.S.A.

Jan D. Miller
Professor
University of Utah
Salt Lake City, UT 84112
U.S.A.

ABSTRACT

The interaction of toner particles in aqueous solution is of interest with regard to both fundamental and practical aspects of de-inking processes. It has been established for the toner studied that the toner polymeric resin, that is, the block copolymer styrene-methyl methacrylate, more specifically the polymethyl methacrylate, has a tremendous influence on the interaction between toner particle surfaces. Interaction force profiles for toners are dependent on the pH conditions, going from attraction to repulsion as the alkalinity of the aqueous medium increases. Both the attraction and repulsion behavior is largely a result of the conformation of polymethyl methacrylate (PMMA) segments. Under strongly acidic conditions the PMMA segments are coiled and toner particles are attracted to each other due to hydrophobic interaction while for alkaline conditions the PMMA segments are more extended into the solution and the toner particles remain dispersed due to steric forces.

INTRODUCTION

Independent of the separation technology used for the de-inking of office waste paper, understanding of toner particle interactions in aqueous systems is important if further advances are to be made in de-inking efficiency. The understanding of such interactions between toner surfaces is not easy due to the complex compositions of toner particles. Toner generally consists of a colorant dispersed in binder resin. Beyond these essential ingredients, a particular toner may contain charge control additives to control the magnitude of the surface charge, surface additives to control flow and cleaning properties, magnetic pigments to aid in toner control, and waxes to promote toner release from the fuser roll. In view of such complex compositions, interaction forces were first measured between pure toner resins such as polystyrene-acrylate to provide a basis for the subsequent analysis of toner/toner interaction force measurements.

The interaction forces for both toner system and polymer systems were measured in different aqueous solutions by using atomic force microscopy (AFM). The use of AFM for the measurement of interparticle force has been described by a number of authors (1-8). Ducker et al. (6,7) were the first to demonstrate the real utility of the AFM the surface force studies when they reported results for the interaction of a silica sphere with a polished silica plate in aqueous electrolyte solutions. Since then the use of AFM for surface force interaction studies has been reported on a wide range of substrates. For quantitative measure of interaction forces it is necessary that first the toner surfaces be well defined in terms of composition and morphology. In this regard, the toner, as well as the toner polymeric resins were characterized and their interaction forces determined.

EXPERIMENTAL

Material

For the experiments the following materials were used, a commercial photocopy toner (see Table I for the composition), polystyrene-methyl methacrylate block copolymer (P(S-*b*-MMA), polymethyl methacrylate (PMMA) and polystyrene (PS).

X-ray Photoelectron Spectroscopy (XPS)

The toners and the copolymer surfaces were analyzed for chemical differences by X-ray photoelectron spectroscopy (XPS) using the XPS equipment at Shell Chemical Company's Westhollow Technology Center- Houston, Texas. With the XPS it is possible to obtain information regarding electronic structure and bonding of atoms in the surface region of 10-200Å.

Atomic Force Microscopy (AFM)

In the present study a Nanoscope IIIa (Digital Instruments) atomic force microscope was used to obtain topographic images and to measure interaction forces.

Topographic image

The topographic images of toner and copolymer surfaces were obtained in the constant deflection mode. Micro-fabricated silicon nitride cantilevers were used for imaging in air with a 5μm scanner. The toner and copolymer topographic images were treated by using the image processing software, version 4.11 (Digital Instrument).

Interaction force

The interaction forces were measured using only a spherical probe and a flat substrate, since with such geometry, the Derjaguin's approximation can be applied to determine the interaction forces involved (9). The colloidal sphere (toner or polymeric resins) was mounted on the tipless AFM cantilever using a speed bonder and an activator by means of a micromanipulator and a CCD camera/monitor system. Extreme care was taken to prevent spreading of the glue on the cantilever tip. In order to assure the adhesion of the sphere on the cantilever, the spherical probes were let to dry for 3 days after gluing.

All the measurements were conducted in the liquid cell. The deflection displacement versus separation distance (sample displacement in z direction) curves were obtained by moving the sample mounted on a piezo crystal along the z-direction towards the sphere surface while monitoring the cantilever deflection. The initial non-linear portion of the deflection displacement vs. separation distance curve represents the change in the net attractive or repulsive force interaction. After contact is established between the sample surface and the sphere, the force curve again becomes linear since the sample on the piezo and the sphere glued on the cantilever move together. The actual force versus separation distance plots were obtained by using the value of 0.12 N/m^2 for the cantilever spring constant and the radius of sphere glued to the cantilever. It should be mentioned that each experiment was repeated at least twice and the forces vs. separation distance curves are an average of at least two repetitions.

RESULTS

Surface Characterization

X-ray photoelectron spectroscopy (XPS)

Due to the toner complexity, the characterization was initially done for just the toner polymeric resin component, the polystyrene-methyl methacrylate block copolymer P(S-*b*-MMA). For both spin coated and cured P(S-*b*-MMA) samples, the XPS wide scan (survey) spectra have shown oxygen (O-1s) and carbon (C-1s) lines, lying at about 532.8 eV and 284 eV respectively. In addition to those lines, another feature present in the spectra is the oxygen Auger line. Table 2 summarizes the elemental composition obtained for these scans. As can be noted, both surfaces have similar composition. Due to the presence of O-1s, it can be said that the PMMA is present on the surface. However, as PS is composed solely of hydrocarbon bonds, it is impossible to confirm its presence by examination of the wide scan spectrum.

Figure 1 shows the C-1s high-resolution spectrum for both P(S-*b*-MMA) samples. From the spectra, it is clear that both PS (π-π^* peak) and PMMA (O-C=O and C-O peaks) are present on the surface. Table 3 summarizes the components of C-1s level. The surface coverage of PS and PMMA was determined by using the peaks, which result from the ionization of both the O-1s and C-1s core levels. The use of the oxygen peaks is straightforward since PS does not contain oxygen. It was assumed that any signal arising from oxygen was due solely to PMMA. The validity of this assumption can be verified by adding up the oxygen functional groups on Table 3; the sum tends to be about the same as the O-1s values in Table 2. The carbon peaks were also used. This was done by recognizing that the total amount of carbon associated with C-H and C-C (backbone) peaks comes from both PS and PMMA, but the contribution of PS is approximately twice as much as that which comes from PMMA. For the calculation the following equation was used $100f_{PS}+50f_{PMMA}$ = %C-H and $f_{PS} + f_{PMMA}=1$, where f_i is the fraction of species i on the surface (10). Table 4 shows the results, using the O-1s and C-1s. As indicated, both methods gave the same results to within less than a few percent difference. Therefore, independent of the sample preparation, it can be said that the copolymer surface consists on the average of 22 percent PMMA and 78 percent PS.

On the basis of these findings, the toner surfaces were analyzed. Table 5 shows the XPS wide scan summary for the photocopy toner A. The toner was analyzed for three different assemblies; commercial, cured and printed on paper. The commercial designation accounts for the toner as received in the cartridge. As indicated in Table 5, besides the presence of O-1s and C-1s lines silicon lines were also detected at approximately 149 eV and at 100eV. It is expected to find silicon on the photocopy toner spectra (Table 1), however the amount of silicon on the printed paper is significantly higher than for the other samples. This silicon enrichment is due to the fact that, the photocopy requires the use of silicone oil to prevent the adhesion of the toner to the roll during fusing. So, it appears that after the printing, some of the silicone oil remains on the toner surface.

Table 6 shows the C-1s high-resolution spectra results for the photocopy toner samples. The interpretation of these results is not straightforward, since other sources besides the P(S-*b*-MMA), such as carbon black, can contribute to the functional groups detected on C-1s. Carbon black is present on the photocopy toner in a range of 10 to 15 percent (Table 1) and typically, it has five major functional groups, carboxylic acids (COOH), phenol (OH), quinone (C=O) and lactones (COO) as well as hydrocarbon bonds. Except for the carboxylic acid and the hydrocarbon groups, common groups for both P(S-*b*-MMA) and carbon black, no additional features are found on the C-1s. Therefore, it is assumed that the photocopy toner surfaces are mainly composed of P(S-*b*-MMA). If this statement is correct, the determination of the surface coverage of PS and PMMA on the toner surface should be close to that values found for P(S-*b*-MMA) samples. Since the O-1s peak arises not only due to P(S-*b*-MMA) but also due to the amorphous silica, the O-1s coverage calculation was based on C-1s oxygen functional groups. Table 7 shows the results for the PMMA coverage on the photocopy toner surfaces. As can be observed, the percentage of PMMA on the toner surface does not shift significantly from the value found for P(S-*b*-MMA) (Table 4). Therefore, it appears that carbon black is not significantly present on the surface. Thus is can be roughly stated that for all surfaces characterized, the copolymer is present in the surface region as 20 percent PMMA and 80 percent PS approximately.

Surface topographic images (morphology)

The morphology of polymers is usually determined by optical and electron microscopy techniques. However, these techniques always require sample preparation in order to isolate the polymer surface, to enhance contrast and to minimize radiation damage. With the atomic force microscopy (AFM) not only is no specimen preparation required, but also it is possible to obtain a three-dimensional surface structure with high resolution in each dimension. In fact, AFM has been applied successfully to the study of homo-polymers and copolymers, specifically for investigation of the structure formation process (11) and the determination of morphological surface structures (12).

The morphology of copolymers is dictated by the relative volume fraction of the homo-polymer blocks that compose the copolymer chain (13,14). If the volume fraction of one component is equal or less than approximately 0.2 then this component forms a body-centered cubic arrangement of spheres in the matrix of the major phase. When the volume fraction of this component increases it forms a series of cylinders, which exhibit hexagonal symmetry, in the major phase. At slightly higher concentration these cylinders form a double diamond-like bicontinuous phase. When

the volume fractions of both components are comparable, then a series of alternating layers of both phases (lamellar morphology) is formed.

Figure 2 shows the AFM images, in contact mode, for P(S-*b*-MMA) spin coated. As can be observed, the copolymer surface exhibits the dispersion of spherical domains. This morphological structure confirms the results found on XPS, where the PMMA is present at 0.2 volume fraction and PS is present at 0.8 volume fraction. Therefore the surface consists of spherical domains of the PMMA component (69.36 nm average diameter) in a PS matrix. In the case of the toner surfaces, the same surface structure involving spherical morphology was also found. Figure 3 shows the AFM image, contact mode, for the photocopy toner.

Interaction Forces

Toner interaction forces

Figure 4 shows the force profiles measured for the toner/toner system, in water, at four different pH values ranging from pH 4.0 to pH 9.0. It can be noticed that the measured forces progress from attraction to repulsion as the water alkalinity increases. These changes in force with pH are typical behavior for systems controlled by electrostatic and van der Waals forces. Of course the van der Waals attraction is independent of pH, but the electrostatic force changes with pH as the toner surface charge is dependent on pH, see Figure 5. In this regard, the measured toner/toner forces were compared to the electrostatic and van der Waals forces (DLVO forces).

The theoretical DLVO force (F/R) between toner surfaces (sphere/plate) was calculated based on the linearized Poisson-Boltzmann equation, the Derjaguin approximation, and van der Waals interactions by the following equation:

$$\frac{F}{R} = \frac{4\pi\sigma_1\sigma_2}{\varepsilon\varepsilon_o\kappa} e^{-\kappa D} - \frac{A}{6D^2} \qquad (1)$$

In Equation 1, σ_1 and σ_2 are the charge densities and for similar surfaces both σ_1 and σ_2 have the same value. ε is the dielectric constant of the medium, ε_o is the permittivity of free space, κ^{-1} is the Debye length , A is the Hamaker constant, and D is the separation distance. The calculation is based on the assumption that the surface charge remains constant as the two surfaces approach one another, since there are large changes of surface potential as the two double layers interpenetrate (15).

Figure 6 compares the theoretical and experimental interaction force (F/R) values. As can be noticed, consideration of only electrostatic and van der Waals forces does not fit the AFM experimental results. In addition, on the basis of this fitting, it is clear that the attraction observed at pH 4, for a separation distance close to 18 nm, is not associated with van der Waals forces. Most likely, this attraction is related to toner interfacial forces, that is, hydrophobic interactions.

Reexamining the force curves for alkaline pH values, it can be observed, for a large separation distance, that the repulsion force is due to the double-layer interaction. However, as the surfaces approach closer, the profile of the force curves has a sharp upturn. This sharp slope is a typical feature of steric repulsion of polymer surfaces (16). In the case of pH 6 and pH 8, this upturn is not so distinct as for pH 9. In order to determine the significance of steric effects, the measured forces in alkaline solution were theoretically compared with both steric and electrostatic forces.

While there is no reason to expected that two toner surfaces interact as two brush layers, it was found that the Alexander-de Gennes equation for the repulsive force between two polymer brush layers describes the steric part of the measured forces very well. Since the Alexander-de Gennes equation is very simple, and because it predicts force profiles that are anyway not very different from those expected for toner surfaces, we used it in our analysis of the results.

Once two brush-bearing surfaces are closer than twice the brush-layer thickness (2L) to each other the repulsive pressure between them is given by (17)

$$P(D) = \frac{kT}{s^3}\left[\left(\frac{2L}{D}\right)^{9/4} - \left(\frac{D}{2L}\right)^{3/4}\right] \qquad (2)$$

In order to get the steric force distance (F(D)) relationship it is necessary to first integrate Equation 2 to obtain interaction free energy W(D) and then use the Derjaguin approximation to obtain F(D):

$$F(D) = 2\pi\ RW(D) = 2\pi\ R\int P(D)dD$$

$$F(D) = \frac{16\pi\ kTL}{35s^3}\left[7\left(\frac{2L}{D}\right)^{5/4} + 5\left(\frac{D}{2L}\right)^{7/4} - 12\right] \qquad (3)$$

So, it should be able to apply Equation 3 to Figure 4 where the interaction is expected to be dominant at short separation distance by steric force. For the large separation distance, the electrostatic force using the same equation applied for the previous computation, that is, the first part on Equation 1, will fit the force curves.

Both electrostatic and steric theoretical equations were separately fitted using, once again, the least squares procedure. Figure 7 shows the result of the fitting with the measured force at different pH conditions. The agreement between the theoretical and experimental results for pH 9 is remarkably good. The force curve was well fitted, at long range with the electrostatic force, while at short separation distance with the steric force. Nevertheless, for the other curves, pH 6 and pH 8, it was impossible to distinguish completely the steric forces from the electrostatic contribution. These results indicate that toner/toner interaction forces are controlled by steric considerations associated with the polymeric components of the toner.

The interaction forces, under discussion, were obtained in water, therefore the dominance of double-layer interaction over the steric forces is obvious. Of course, by adjusting the ionic strength of the medium, the electrostatic contribution can be screened out and the steric forces can prevail. By increasing the salt concentration of the solution, for instance at pH 6, what is observed is that the steric forces become progressively dominant. The interaction force goes from attraction (0M KCl) to monotonically repulsive as the concentration of KCl increases. See Figure 8.

Since toner has a complex composition, it is difficult to be certain if all force profiles observed so far are related only to the toner polymeric composition. In this regard, it is reasonable, at this point, to consider the interaction forces for only the toner (P(S-*b*-MMA)) copolymer.

Polystyrene-methyl methacrylate (P(S-*b*-MMA)) interaction forces

Figure 9 shows the measured forces for the P(S-*b*-MMA)/P(S-*b*-MMA) system in water at different pH values. These forces are similar to the profiles found for the toner/toner system. At pH 4, the P(S-*b*-MMA) surfaces undergo attraction at a separation distance around 39 nm. In this case, the magnitude of the attraction distance was twice the value obtained for toner/toner interaction. This difference might be related to the fact that in toner the P(S-*b*-MMA) is diluted by other components of the toner.

The alkaline force profiles also have the same trends as observed for toner/toner interaction. However, for the P(S-*b*-MMA)/ P(S-*b*-MMA) system, the steric contribution is more discernible. See the sharp slope at short separation distances. The steric and electrostatic fitting, for the P(S-*b*-MMA) curves, is shown in Figure 10. These results indicate that, the alkaline measured forces can be fitted very well by a steric repulsion at short range together with the double-layer repulsion at larger separation distances.

From the results of Figure 8, the electrostatic contribution can be fully screened from the force profile in the presence of 0.1 M KCl. In this regard, the steric interaction between P(S-*b*-MMA)/ P(S-*b*-MMA) was investigated at such salt concentration. See Figure 11. As can be observed, the attraction at pH 4 is achieved at a shorter separation distance (13 nm) while at pH 6, the interaction is entirely repulsive. The conversion of attraction to repulsive interaction with an increase in the salt concentration at pH 6 can be explained as follows. In water, the polymer segments are extended from the surface as can be seen by the sharp upturn of the curve before the jump to contact. Most likely, at pH 6, the extended segments are not strongly charged. So with a closer approach, the segments attract each other due to van der Waals or hydrophobic interactions. In the presence of KCl, it is feasible that the polymer segments adsorb Cl^- ions and as a result the segments become ionized. Therefore, at closer approach, the segments have a tendency to be repelled from each other due to Coulombic repulsion. Figure 12 shows the steric and electrostatic fitting for the 0.1 M KCl alkaline force curves. The agreement between the theory and experiment is again very good.

Considering that both toner and P(S-*b*-MMA) show the same trends for the force profiles, it is concluded that the P(S-*b*-MMA) is responsible for the toner/toner interaction behavior. From AFM topography image analysis, it is known that spherical domains of PMMA are exposed at the surface of PS matrix. Therefore, it is presumed that the PMMA protrusions are responsible for the force profiles observed so far. In this regard the PMMA/PMMA interaction is of interest.

Polymethyl methacrylate (PMMA) interaction forces

As expected, the measured force curves for PMMA/PMMA in water at different pH values behave the same as the toner/toner and P(S-*b*-MMA)/ P(S-*b*-MMA) systems. See Figure 13. Once more, attraction is observed at pH 4, and occurs close to 44 nm. The absence of repulsion at pH 4, for all systems studied, is an indication that the polymer segments are coiled. Figure 14 shows the PMMA measured zeta potential as a function of pH. As can be noticed, at pH 4, PMMA has a relatively high potential of – 30 mV in water. Nevertheless, if this potential is compared with the one at pH 6 (-51 mV) or even with the one at pH 8 (-71 mV), then the PMMA potential value of –30 mV is pretty low. On the basis of the force curve and zeta potential measurements, it can be said that the PMMA segments rather prefer to interact with themselves and remain coiled rather than to extend into solution at pH 4.

With respect to the PMMA alkaline curves, not much needs to be mentioned since they are very similar to the ones found for P(S-*b*-MMA), that is, the force curves goes from electrostatically-dominated at long separation distances to sterically-dominated at short separation distances. Figure 15 shows the steric and electrostatic fitting for the alkaline curves. The same trends are found. The curves are well fitted with both steric and electrostatic forces.

Following the same procedure, Figure 16 shows the PMMA force curve in 0.1 M KCl solution. With no surprises, the force curves show the same profile as for toner and P(S-*b*-MMA) and the fit is remarkable. See Figure 17. Since all data presented above agree reasonably well with the data found for P(S-*b*-MMA)/ P(S-*b*-MMA) and toner/toner systems, it is concluded that PMMA is the polymer controlling the steric repulsive force.

Polystyrene (PS) interaction forces

Although the results above have confirmed that the PMMA is responsible for the interaction behavior of these toner/toner systems, it will be more conclusive to verify such findings by analysis of the polystyrene/polystyrene system. Figure 18 shows the force curves for polystyrene/polystyrene interaction, in water, at different pH values. As can be observed, independent of the pH, the force curves are all attractive. The surfaces attracts each other at separation distances 26.7 nm for pH 9, 26.9 nm for pH 8 and 22.4 nm for pH 6. The magnitudes of the attractive separation distance suggest that the interaction between polystyrene surfaces is hydrophobic. This finding, were in agreement with the results reported in the literature for the polystyrene/polystyrene interaction (18, 19).

Comparing the force curves of polystyrene with the ones for toner and P(S-*b*-MMA), it is clear that the PMMA is the polymer responsible for the interaction profile of toner particles.

SUMMARY AND CONCLUSIONS

From the toner characterization, it has been determined that the toner surface consist of spherical domains of polymethyl acrylate – PMMA (0.2 volume fraction) in a matrix of Polystyrene – PS (0.8 volume fraction). This finding has significant importance for the understanding and interpretation of interaction force curves obtained by AFM.

It has been demonstrated that the interaction forces between toner particles are controlled by the polymeric composition of the toner. For the photocopy toner studied, the interaction is ruled by the block copolymer polystyrene-methyl methacrylate, more specifically by the polymethyl-methacrylate (PMMA). The force profiles are dependent of the pH conditions, going from attraction to repulsion as the alkalinity of the medium increases. Attractive interactions are observed between toner particles in acidic solutions. Such attraction is a result of the conformation of PMMA segments. At acidic pH values, the PMMA segments rather prefer to interact between themselves than to be extended from the surface, leading to coiling of the segments. When the toner surfaces come closer no resistance is offered and the surfaces undergo attraction. Under alkaline conditions the interaction is repulsive once again due to the conformation of the PMMA segments. The alkalinity of the medium extends the PMMA segments into the solution. With the approach of the surfaces, the segments overlap, leading to a repulsive osmotic force due to the unfavorable entropy associated with compression of the segments. This repulsive steric interaction opposes any attractive force and thus the toner particles are push apart. The toner interactions are also influenced by the salt concentration of the medium. In fact salt has a paradoxical effect on the force profile. It helps to establish the steric force by screening out the electrostatic contribution but at same time is a poor solvent for PMMA and hence the magnitude and range of the steric force is reduced.

ACKNOWLEDGMENTS

The authors gratefully acknowledge the financial support provided by NSF (CTS-9215421 and CTS-9618582). Also thanks is extended to the Xerox Corporation for the toner and toner polymeric resin samples and to the Shell Chemical Company, particularly Dr. John Borchardt, for the XPS analysis.

REFERENCES

1. Binning G., Quate, C. F., and Geber, C., Phys. Rev. Lett. 56, pp. 930 (1986).

2. During, U., Gimzewskii, J. K., and Pohl, D. W., Phys. Rev. Lett., 57, pp. 2403 (1986).

3. Goodman, F. O., and Garcia, N., Phys. Rev. B, 43 pp.4728 (1991).

4. Hartmann, U., Phys. Rev. B, 43, pp. 2404 (1191).

5. Butt, H.-J., Biophys. Journal, 60, pp.1438 (1991).

6. Ducker, W. A., Senden, T. J., and Pashley, R. M., Nature, 353, pp.239 (1991).

7. Ducker, W. A., Senden, T. J., and Pashley, R. M., Langmuir, 8, pp.1831 (1992).

8. Larson, I., Drummond, C. J., Chan, D. Y. C., and Griese, F., J. Am. Chem. Soc., 115, pp.11885 (1993).

9. Derjaguin, B. V., Kolloid Z., 69, pp.155 (1934).

10. Green, P. F., Christensen, T. M., Russell, T. P., and Jérôme, R., Macromolecules, 22, pp.2189 (1989).

11. Collin, B., Chatenay, D., Coulon, G., Ausserre, D., and Gallot, T., Macromolecules, 25, pp.1624 (1992).

12. Annis, B. K., Schwark, D. W., Reffner, J. R., Thomas, E. L., and Wunderlich, B., Makromol. Chem., 193, pp.2589 (1992).

13. Woodward, A. E., "Atlas of Polymer Morphology", Hanser Publisher: New York, pp.189 (1989).

14. Sawyer, L. C., and Grubb, D. T., "Polymer Microscopy", Chapman & Hall: London, 1987.

15. Li, Y. Q., Tao, N. J., Garcia, A. A., and Lindsay, S. M., Langmuir, 9, pp.637 (1993).

16. Kamiyama, Y. and Israelachvili, J., Macromolecules, 18, pp. 721 (1985).

17. de Gennes, P. G., C. R. Acad. Sci., 300, pp.839 (1985).

18. Christenson, H. K., and Yamisky, V.V., Colloid Surf. A: Phys. Eng. Aspects, 129-130, pp.67 (1997).

19. Karaman, M. E., Meagher, L., and Pashley, R. M., Langmuir, 9, pp.1220, (1993).

Table 1. Toner composition as determined from the material safety data sheet (MSDS)

Toner	Composition
Photocopy toner	Styrene/acrylate Copolymer (85-90%) Carbon Black (10-15%) Amorphous Silica (< 1%) Zinc Stearate (< 1%)

Table 2. XPS wide scan summary for composition of polystyrene-methyl methacrylate P(S-*b*-MMA) surfaces.

Sample	C-1s	O-1s	O/C
Spin Coated	91.60	8.31	0.09
Cured	91.27	8.73	0.10

Table 3. XPS C-1s chemical shifts for polystyrene-methyl methacrylate P(S-*b*-MMA) surfaces.

	Functional Groups				
Sample	C-H	C-C	O-C	O-C=O	π-π^*
Spin Coated	77.22	12.08	4.56	3.66	2.47
Cured	77.30	11.78	5.43	3.27	2.22

Table 4. Relative percent of polymethyl methacrylate (PMMA) on P(S-*b*-MMA) Surfaces.

Sample	Calculated from O-1s peaks (O-C=O, C-O)	Calculated from C-1s peaks (C-H and C-C)
Spin Coated	21.87	21.40
Cured	22.97	22.89

Table 5. XPS wide scan summary for composition of photocopy toner surfaces.

Sample	C-1s	O-1s	Si-2p	O/C
Commercial	71.44	20.16	8.40	0.28
Cured	75.56	18.78	5.66	0.25
Printed Paper	66.57	19.21	14.22	0.29

Table 6. XPS C-1s chemical shifts for the photocopy toner surfaces.

	Functional Groups				
Sample	C-H	C-C	O-C	O-C=O	π-π^*
Commercial	74.82	13.11	4.76	4.08	3.22
Cured	74.81	14.88	5.98	3.39	0.94
Printed Paper	77.97	14.23	4.22	2.32	1.26

Table 7. Relative percent of polymethyl methacrylate (PMMA) for the photocopy toner surfaces.

Sample	Calculated from C-1s peaks (O-C=O, C-O)	Calculated from C-1s peaks (C-H and C-C)
Commercial	23.26	24.14
Cured	24.66	20.62
Printed Paper	17.21	15.60

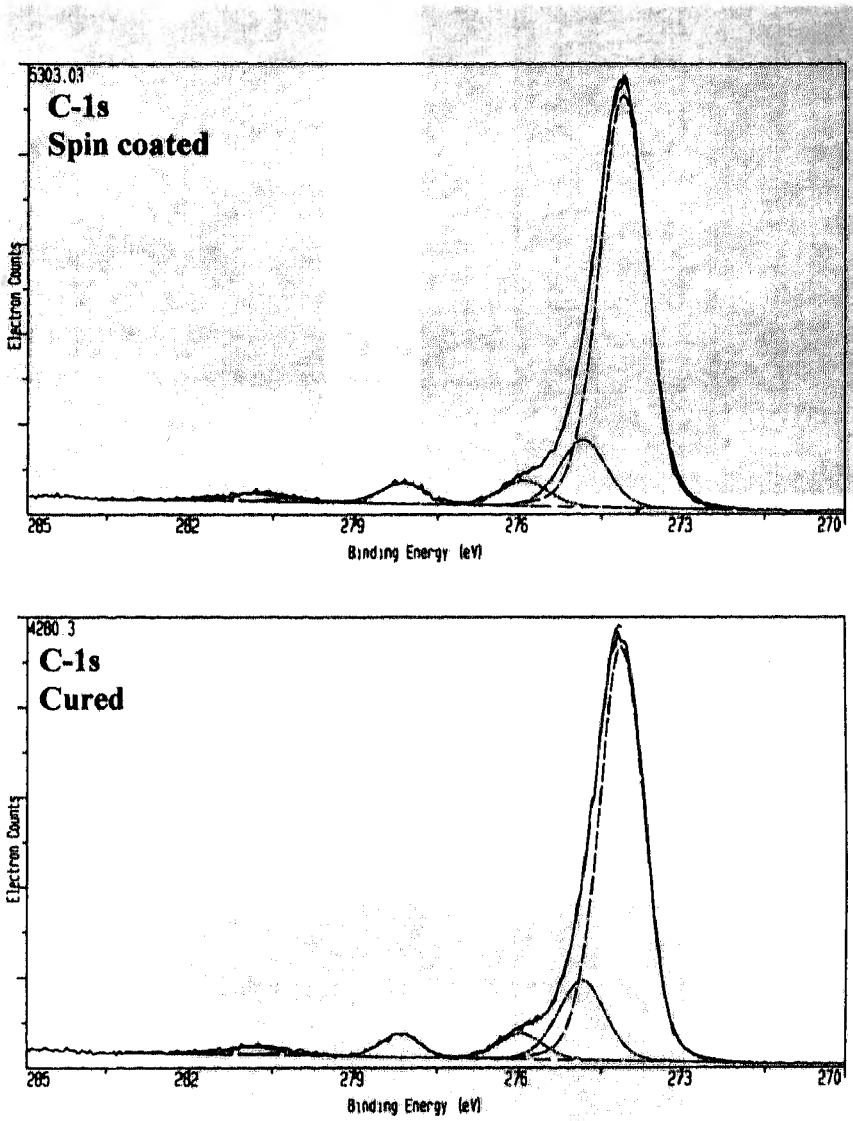

Figure 1 – C-1s spectra for the block copolymer polystyrene-methyl methacrylate P(S-*b*-MMA).

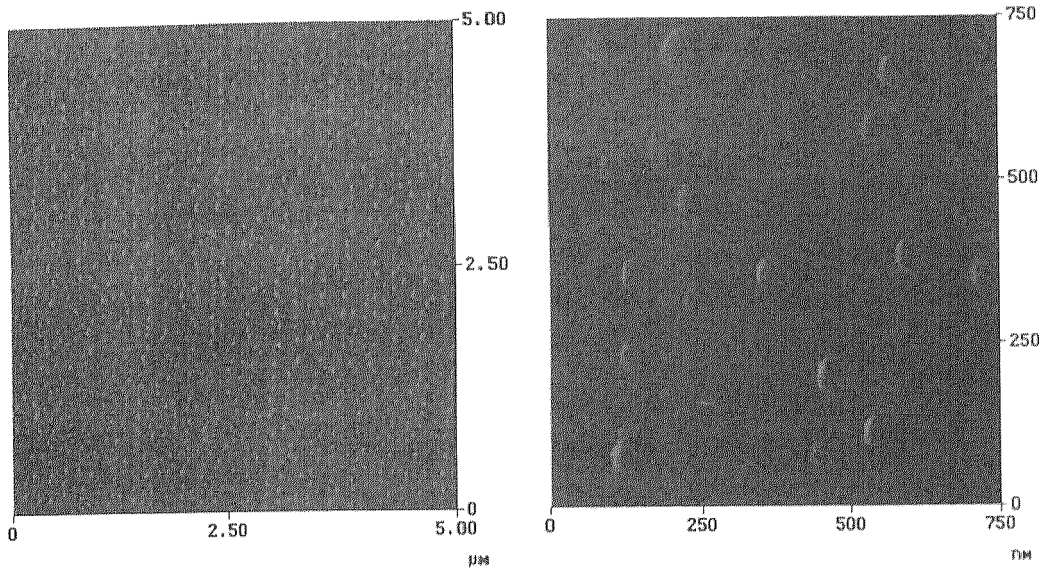

igure 2 – AFM images, contact mode, for P(S-*b*-MMA) spin coated.

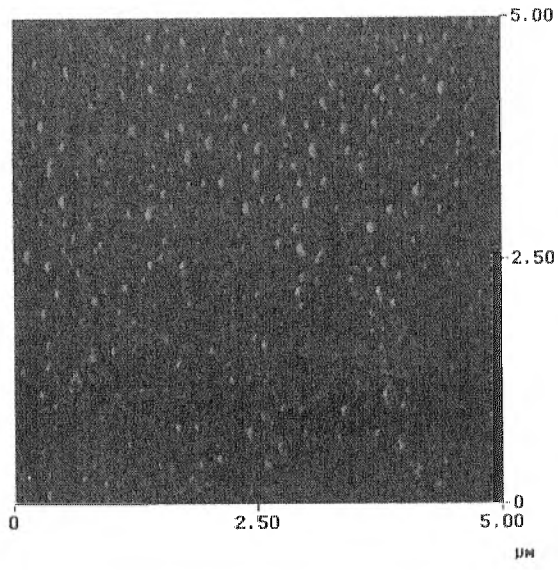

Figure 3 – AFM images, contact mode, for the cured photocopy toner

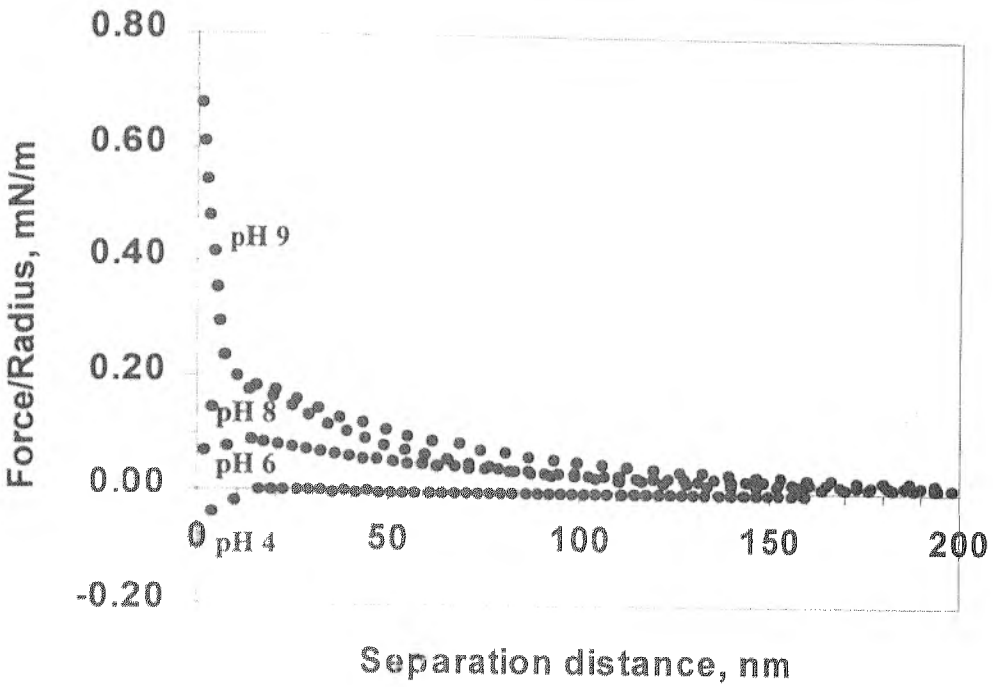

Figure 4- Interaction force profiles between toner surfaces in water at different pH values.

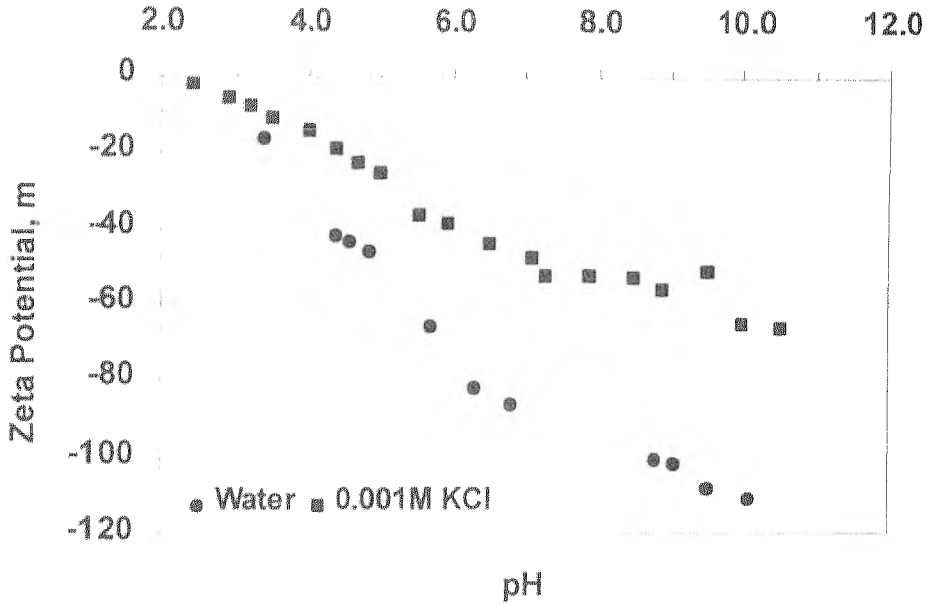

Figure 5 – Zeta potential for the photocopy toner.

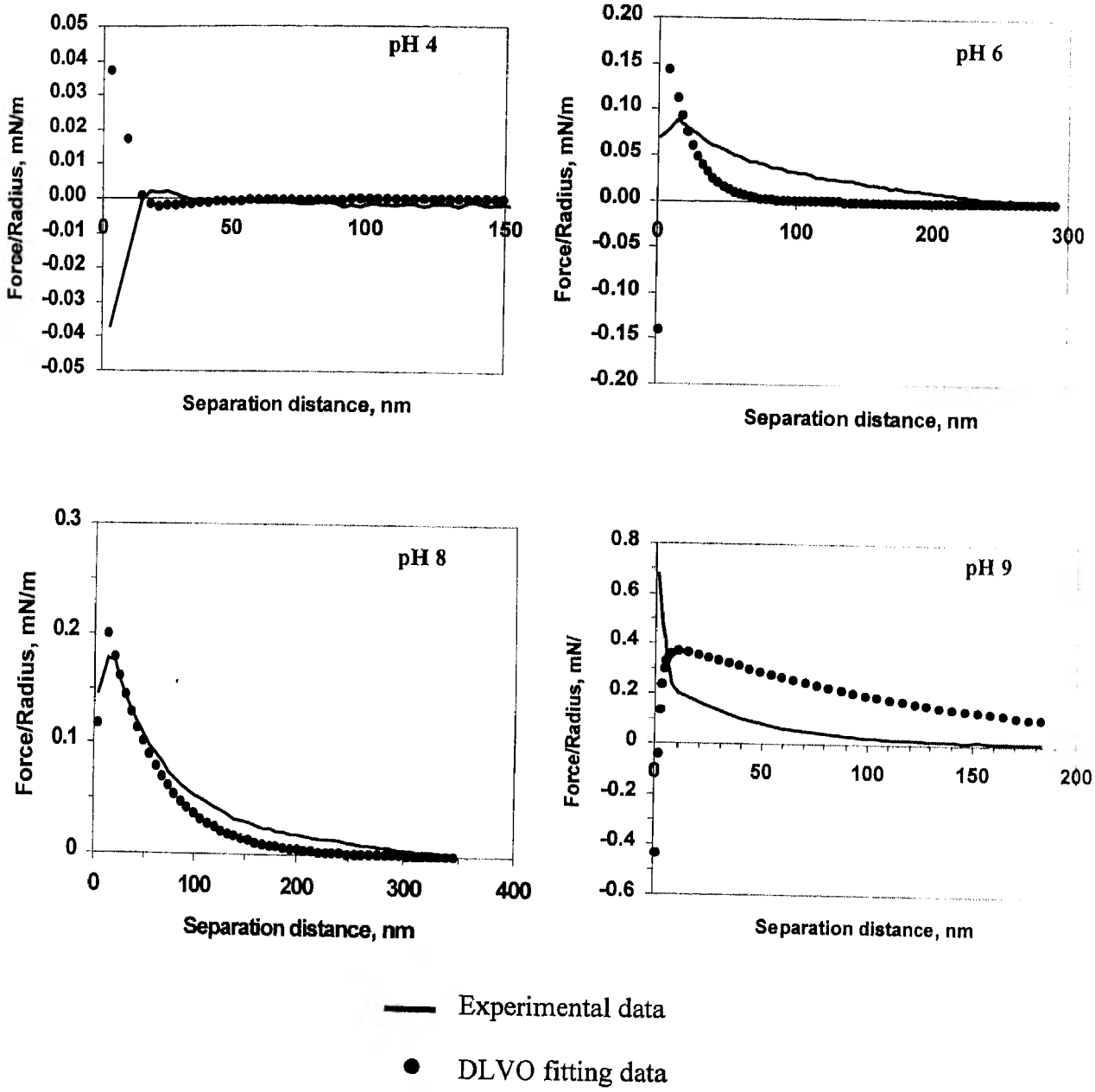

Figure 6 – DLVO fitting for toner–toner experimentally measured forces at different pH values.

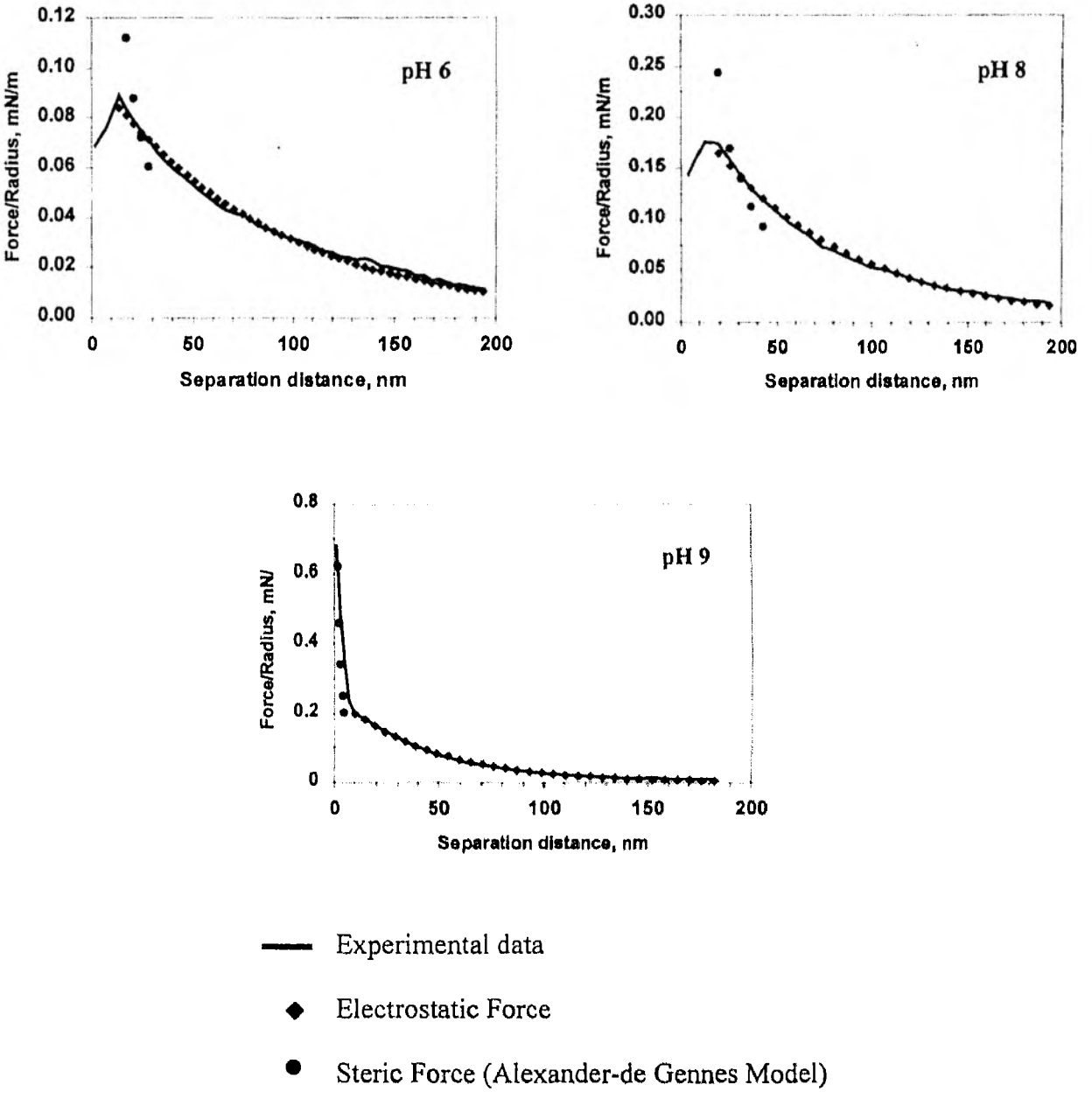

Figure 7 – Toner-Toner interaction force, in water at different pH values, fitted with electrostatic and steric force models.

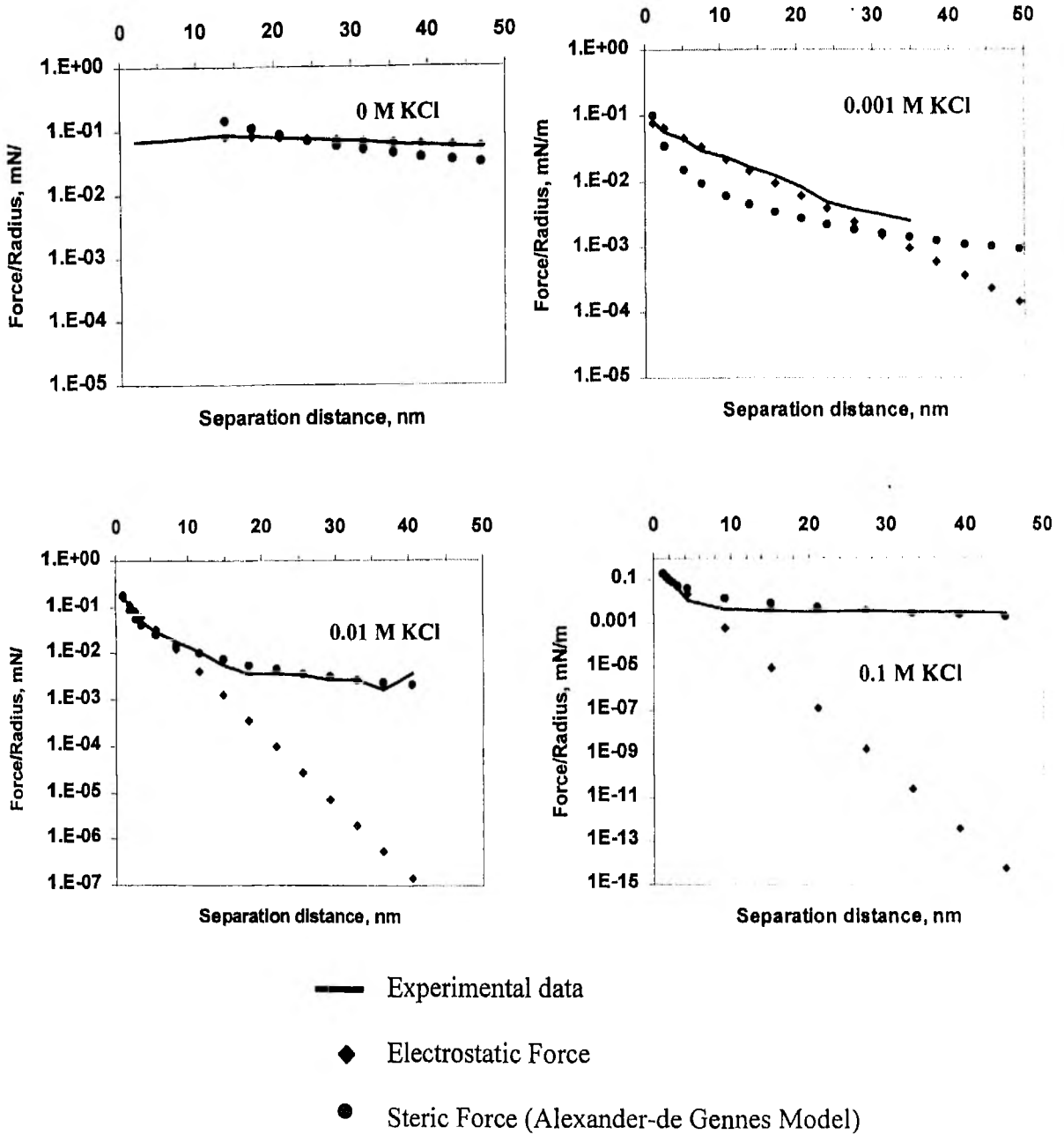

Figure 8 – Effect of salt concentration on toner-toner interaction force at pH 6.

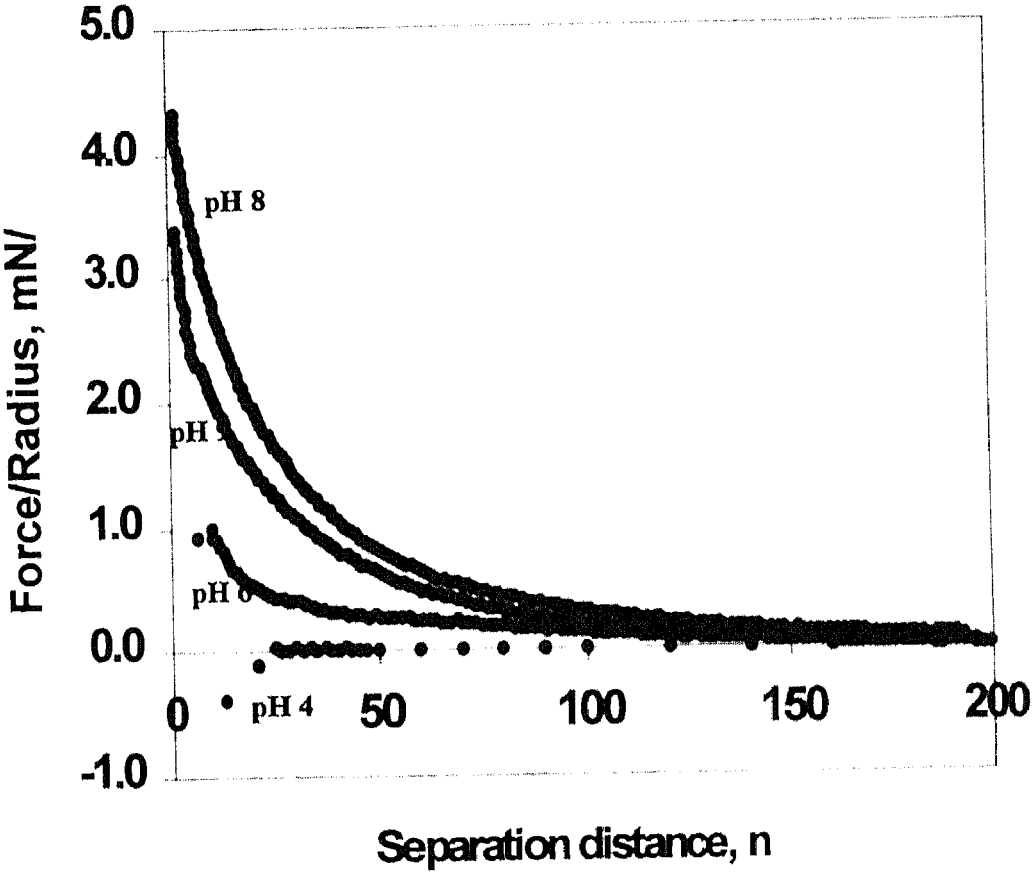

Figure 9- Experimental force profiles for polystyrene-methyl methacrylate P(S-*b*-MA) surfaces in water at different pH values.

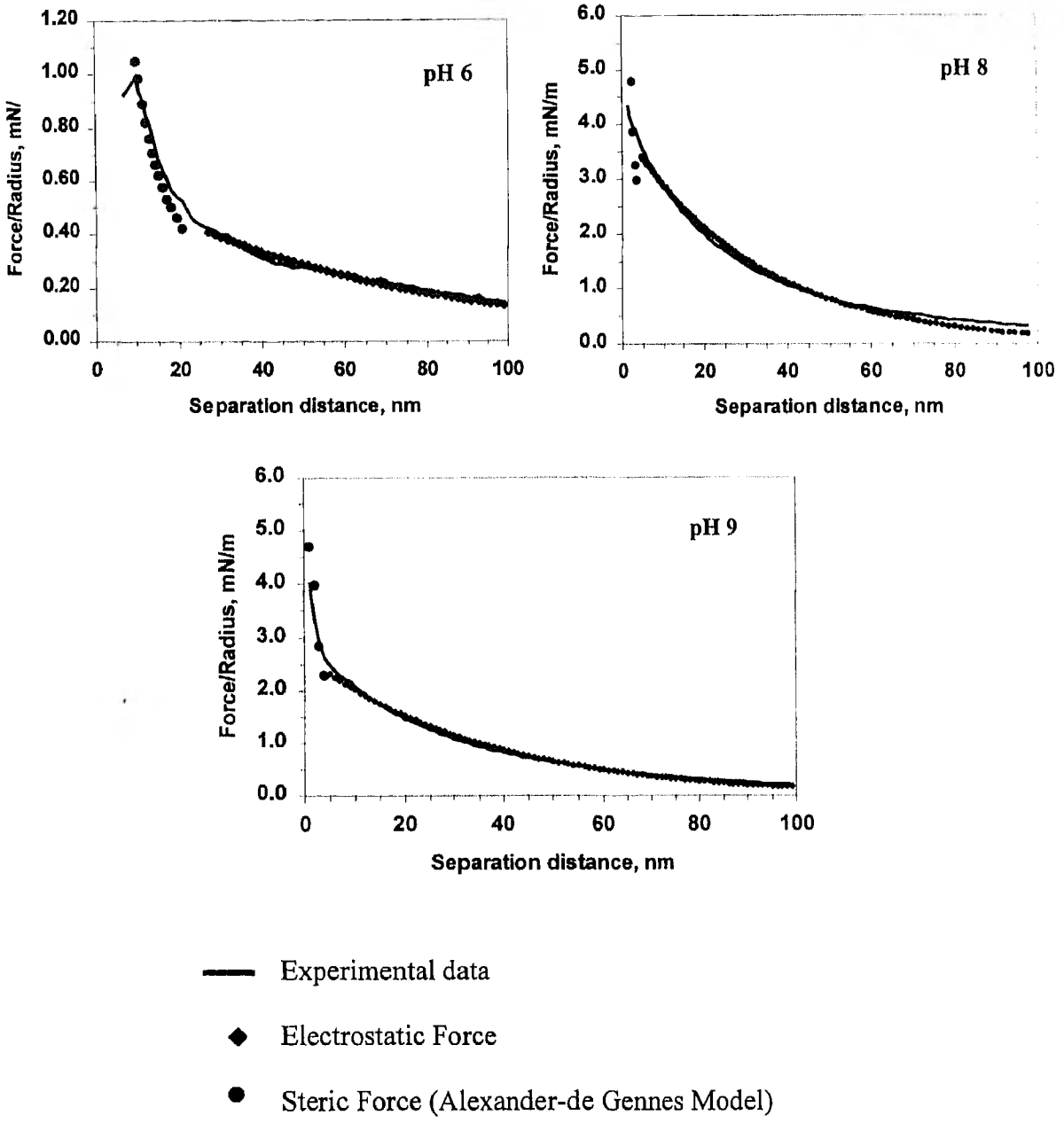

Figure 10 – P(S-*b*-MMA)-P(S-*b*-MMA) interaction forces, in water at different pH values, fitted with electrostatic and steric force models.

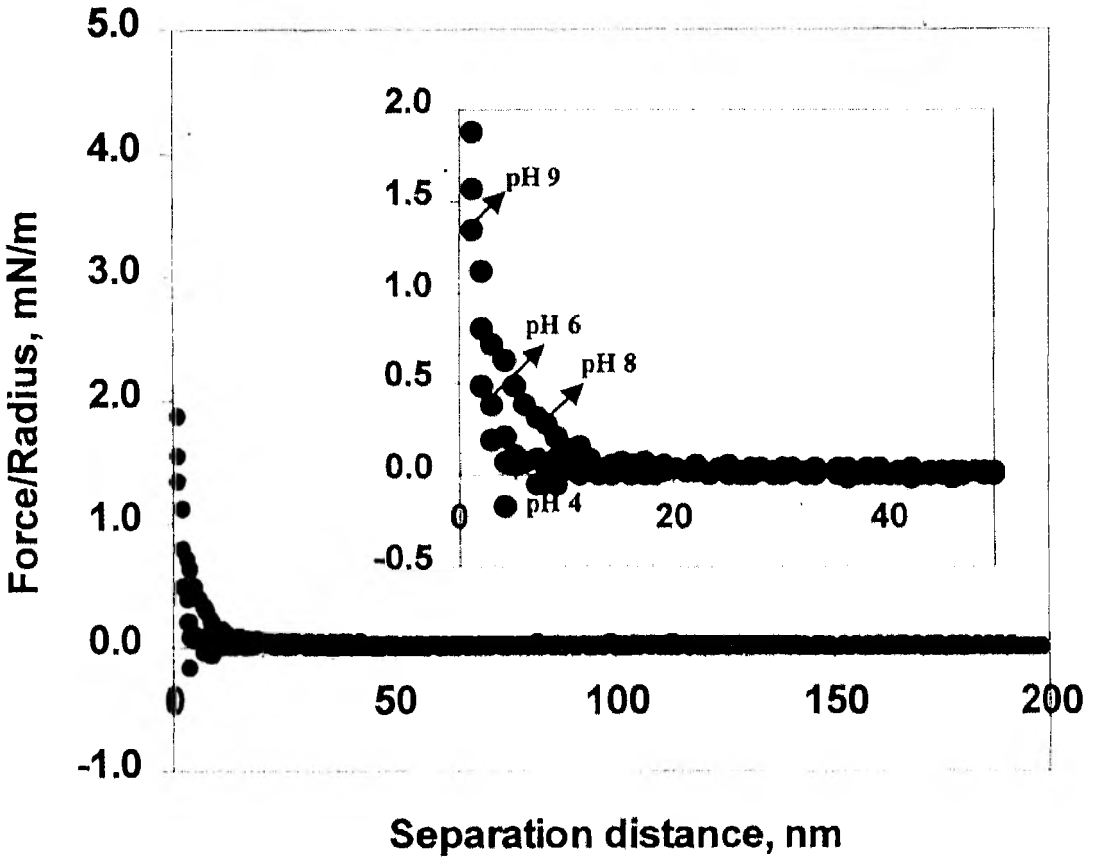

Figure 11- Experimental force profiles between copolymer polystyrene-methyl methacrylate P(S-*b*-MMA) surfaces in 0.1M KCl at different pH values.

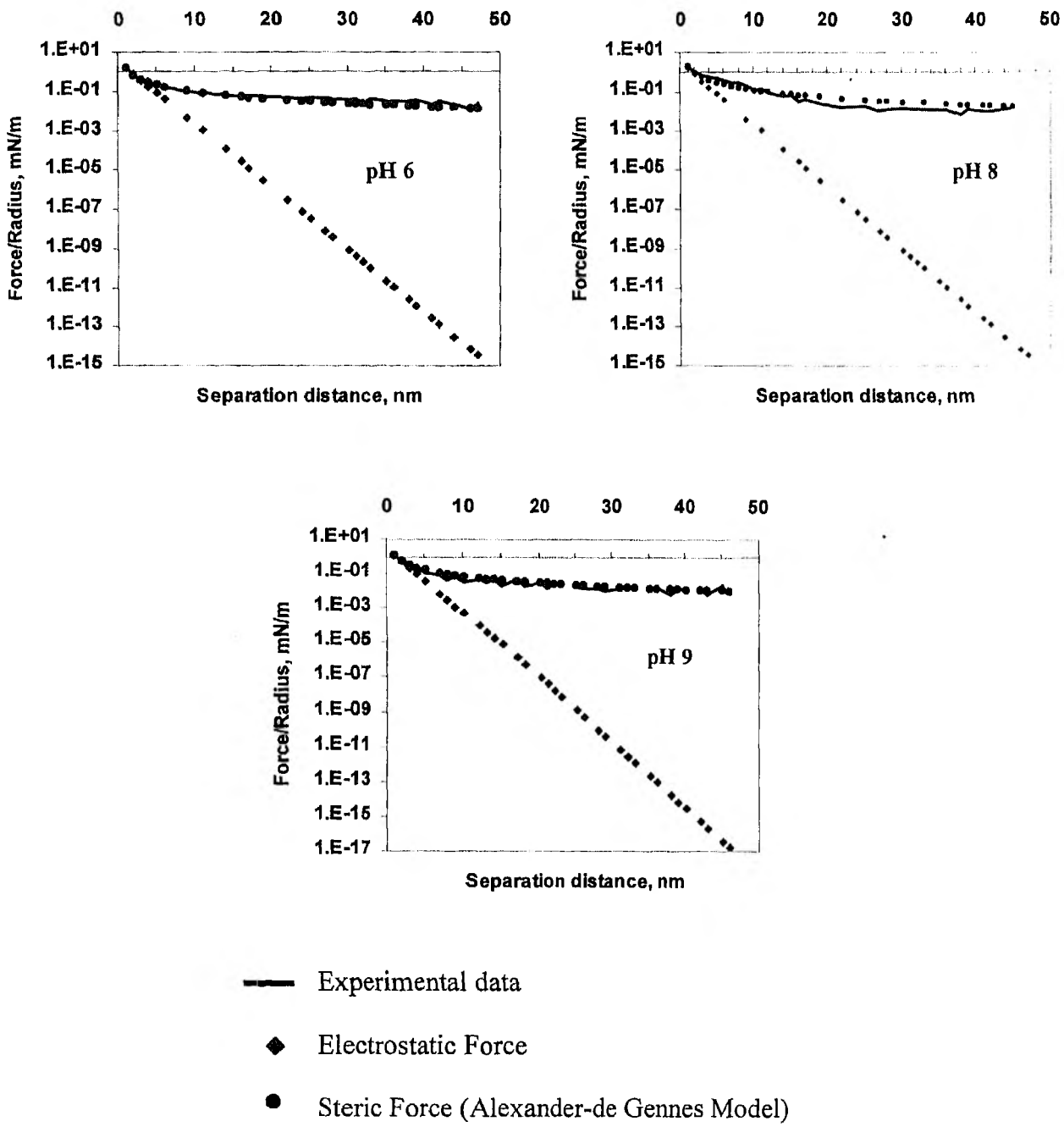

Figure 12 – P(S-*b*-MMA)-P(S-*b*-MMA) interaction forces, in 0.1 M KCl at different pH values, fitted by electrostatic and steric force modes

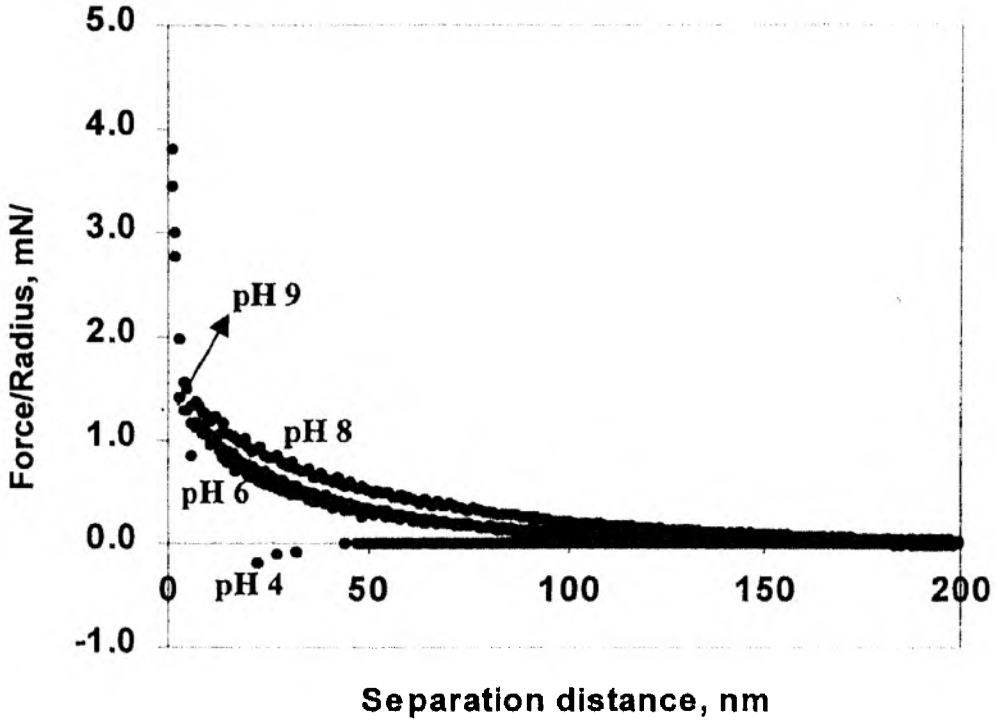

Figure 13 – Experimental force profiles between polymethyl methacrylate (PMMA) surfaces in water at different pH values.

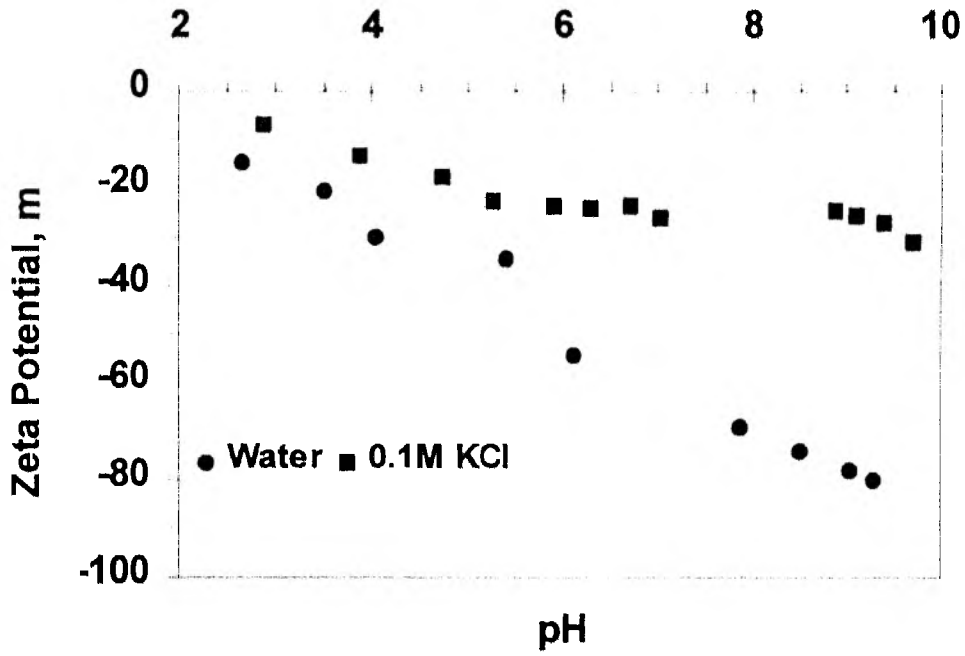

Figure 14 – Zeta potential for polymethyl methacrylate (PMMA)

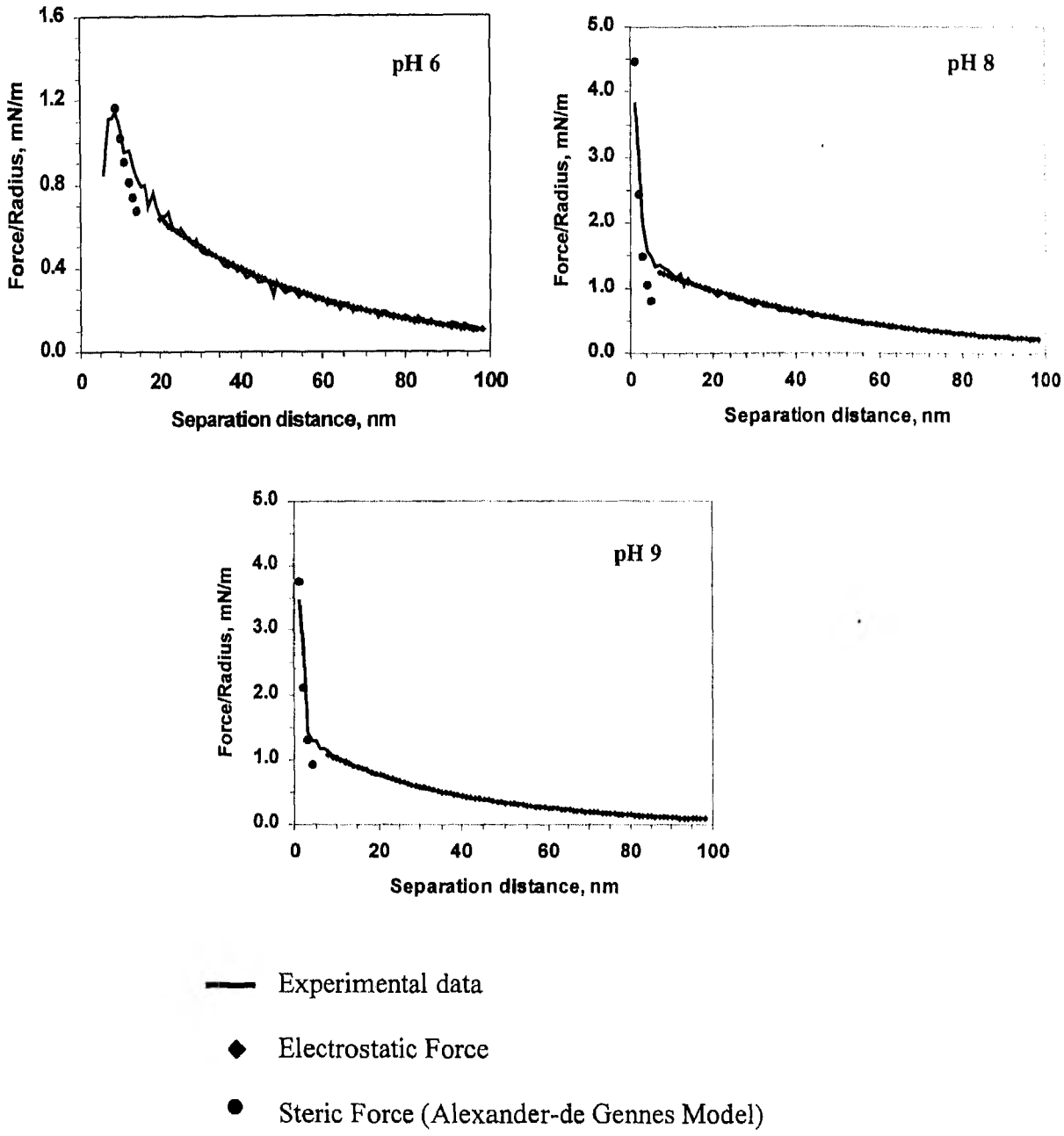

Figure 15– PMMA-PMMA interaction forces, in water at different pH values, fitted by electrostatic and steric force models.

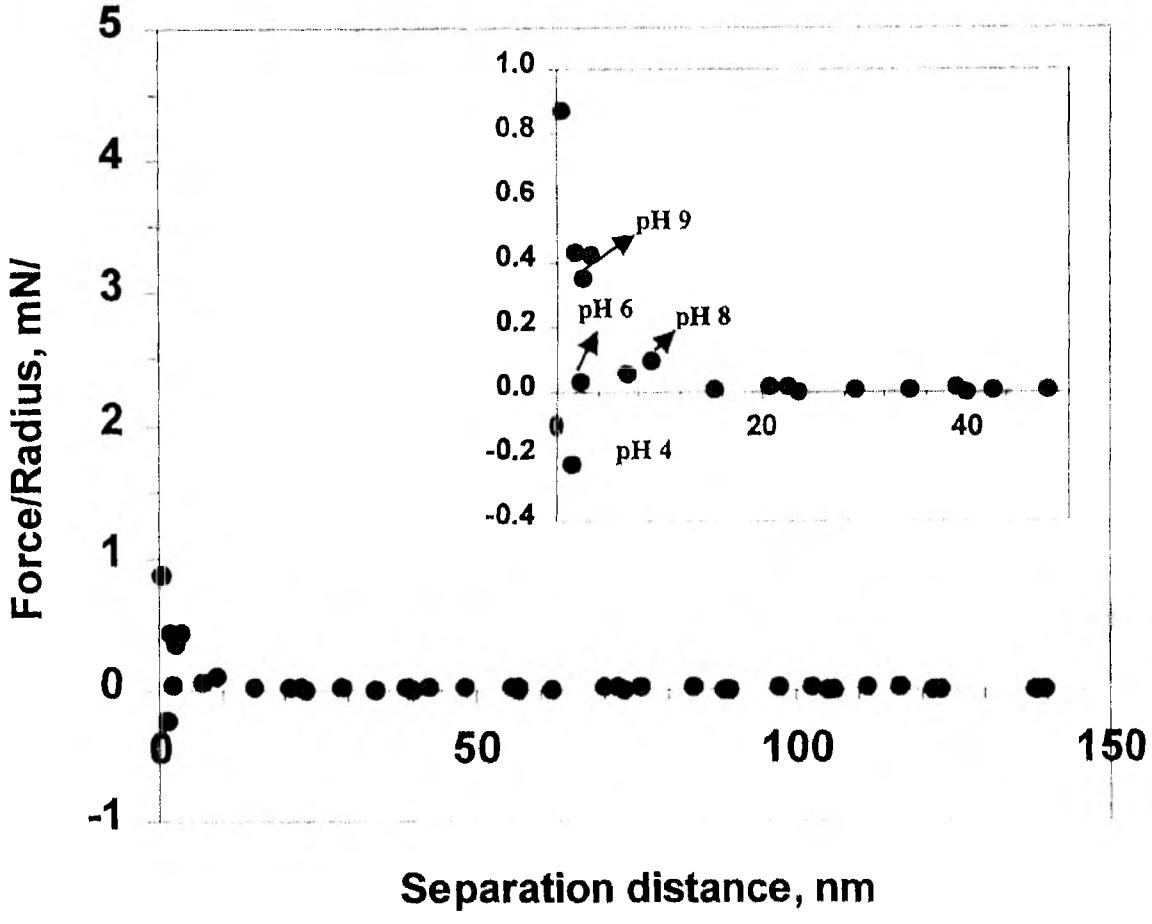

Figure 16-Experimental force profiles between polymethyl methacrylate (PMMA) surfaces in 0.1M KCl at different pH values.

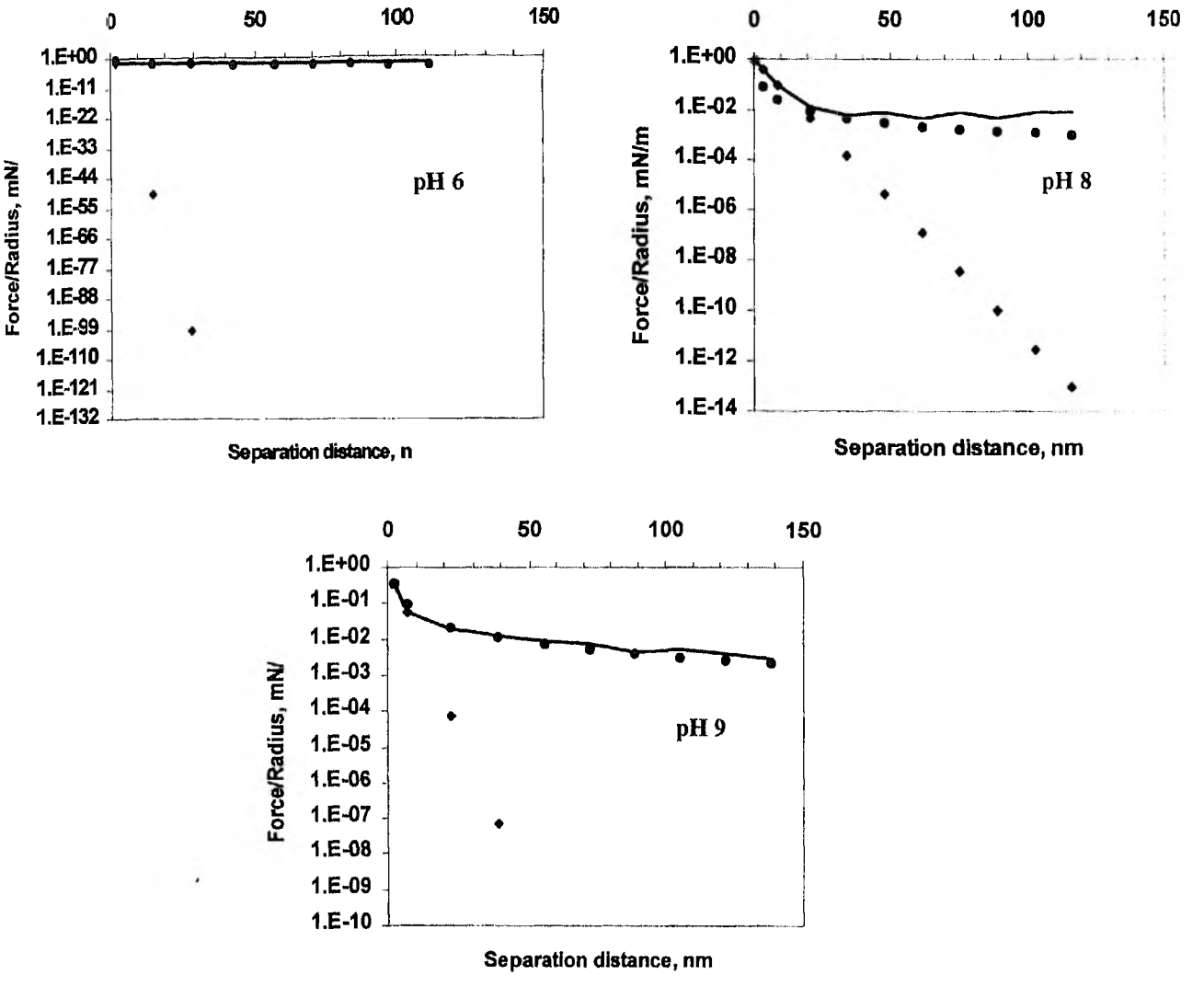

Figure 17 – Logarithm of PMMA-PMMA interaction forces, in 0.1 M KCl at different pH values, fitted by electrostatic and steric force models.

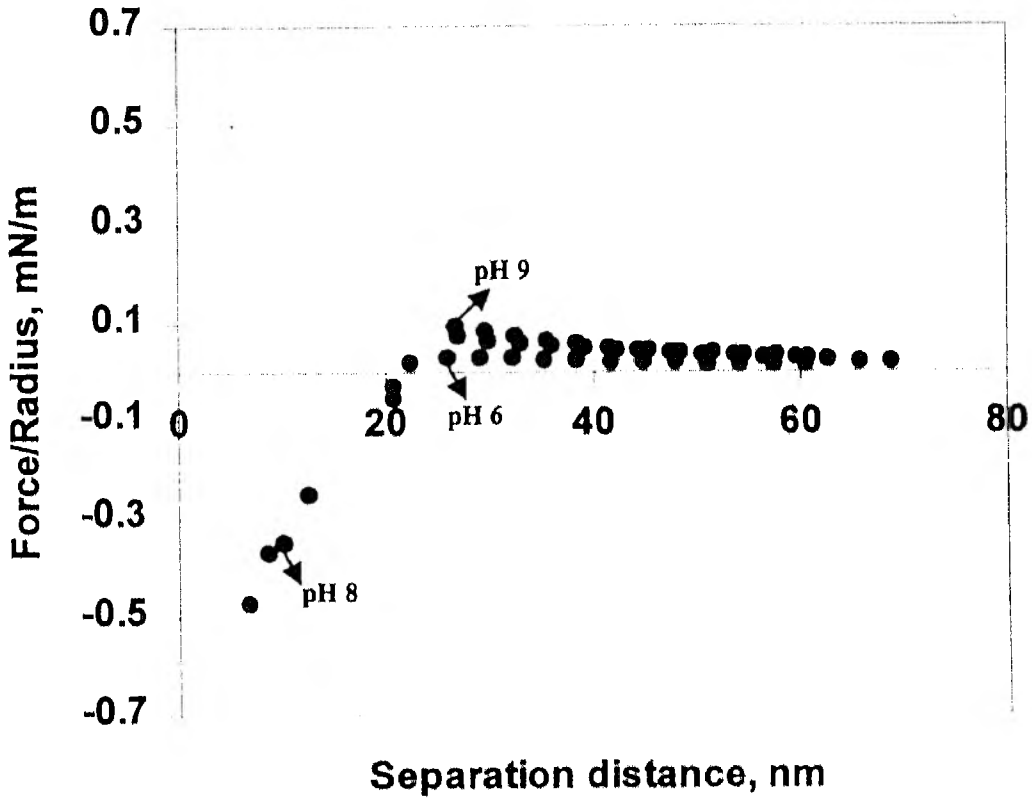

Figure 18 – Experimental force profiles between polystyrene (PS) surfaces in water at different pH values.